Development of an anti-tauopathy mucosal vaccine specifically targeting pathologic conformers

Joon Haeng Rhee (jhrhee@chonnam.ac.kr)
Chonnam National University https://orcid.org/0000-0003-4018-3203

Wenzhi Tan
Chonnam National university

Jayalakshmi Thiruppathi
Chonnam National university

Seol Hee Hong
Chonnam National university

Sao Puth
Royal University of Phnom Penh https://orcid.org/0000-0002-3792-9505

Sophea Pheng
Chonnam National university

Bo-Ram Mun
Chonnam National university

Won-Seok Choi
Chonnam National university

Kyung-Hwa Lee
Chonnam National university

Hyun-Sun Park
Chonnam National university

Duc Nguyen
Chonnam National University

Min-Cheol Lee
Chonnam National university

Kwangjoon JEONG
Chonnam National University https://orcid.org/0000-0001-9413-6934

Jin Hai Zheng
Chonnam National university

Young Kim
Chonnam National university

Shee Eun Lee
Chonnam National University https://orcid.org/0000-0002-2023-3317

Article

Keywords:

Posted Date: December 11th, 2023

DOI: https://doi.org/10.21203/rs.3.rs-3686019/v1

Additional Declarations: (Not answered)

Abstract

Alzheimer's disease (AD) and related tauopathies are associated with pathological tau protein aggregation, which plays an important role in neurofibrillary degeneration and dementia. Immunotherapy targeting and resolving the pathological tau aggregates is known to improve cognitive deficits in AD animal models. The repeat domain of tau (TauRD) plays a pivotal role in tau-microtubule interactions and is critically involved in the aggregation of hyperphosphorylated tau proteins. Considering that TauRD forms the structural core of tau aggregates, the development of immunotherapy selectively targeting TauRD-induced pathological aggregates holds great promise for the modulation of tauopathies. In this study, we generated a recombinant TauRD polypeptide forming neurofibrillary tangle (NFT)-like structures and evaluated TauRD-specific immune responses following intranasal immunization in combination with the mucosal adjuvant FlaB. In BALB/C mice, repeated immunizations at one-week intervals induced robust TauRD-specific antibody responses in a TLR5-dependent manner. Notably, the resulting antiserum recognized only the aggregated form of TauRD, while ignoring monomeric TauRD. The antiserum effectively inhibited TauRD filament formation and promoted phagocytic degradation of TauRD aggregate fragments by microglia. The antiserum could also specifically recognize pathological tau conformers in the human AD brain. Based on these results, we engineered a built-in flagellin-adjuvanted TauRD (FlaB-TauRD) vaccine and tested the vaccine efficacy in a P301S transgenic mouse model. Mucosal immunization with FlaB-TauRD improved quality of life, such as memory deficits, and ameliorated tauopathy progression. More notably, the survival of the vaccinated mice was dramatically extended. Conclusively, we have developed a mucosal vaccine exclusively targeting pathological tau conformers and preventing disease progression.

One Sentence Summary

A built-in flagellin-adjuvanted vaccine targeting pathologic tau protein structure prevented tauopathy progression and extended survival.

INTRODUCTION

Tauopathies are a class of neurodegenerative diseases associated with pathological aggregation of microtubule (MT)-associated tau protein in the human brain, leading to neurofibrillary degeneration and dementia [1–3]. Alzheimer's disease (AD), a secondary tauopathy, is the most common cause of dementia affecting more than 35 million people [4–6]. AD is tightly related to insoluble hyperphosphorylated tau aggregates, which will consequently form neurofibrillary tangles (NFTs) [7]. In addition to an intraneuronal accumulation of tau NFTs, another classical hallmark of AD is interneuronal amyloid-β (Aβ) deposition [8, 9]. The Aβ amyloid cascade hypothesis claims that Aβ deposition in the brain initiates the disease process accompanying NFT formation and represents the first neurotoxic insult [10, 11]. However, clinical trials aimed at reducing Aβ levels have failed or showed limited efficacy in improving cognition, highlighting the need for alternative targets [12]. The accumulation of NFTs and the transcytosis-mediated spread of NFTs in the brain are more directly correlated with neuronal loss and the

progressive cognitive decline in AD [13, 14]. Hence, preventive and therapeutic approaches targeting tau pathology progression would serve as promising alternatives [15]. More than 30 drugs interfering with the aggregation, processing, and accumulation of tau reached the clinic during the last two decades without notable clinical efficacy [16].

Interest in tau-targeted immunotherapy is growing immensely in the AD field. The first vaccination approach in wild-type mice using full-length tau protein emulsified in complete Freund's adjuvant resulted in tauopathy-like abnormalities and encephalitis [17]. On the other hand, active and passive immunotherapies targeting phospho-epitopes of tau or tau aggregates have been reported to effectively reduce tau pathologies and improve cognitive performances in transgenic animal models [18–22]. However, AD brain tissues contain paired helical filaments (PHFs) with phosphorylation at numerous serine, threonine, and tyrosine residues and multiple post-translational modifications [23]. Targeting a limited number of phosphorylated domains may result in insufficient coverage. Moreover, those phospho-tau epitopes are also found in physiological tau proteins [24]. In this regard, sarkosyl-insoluble PHF-tau, representing tau pathologic conformers, had been experimentally tested in an aged tau-transgenic mouse model [25]. Even insoluble PHF-tau prepared from pathologic tauopathy tissue would still carry a risk of inducing autoimmune reactogenicity after vaccination. In this context, we hypothesized that the pathological conformation only formed by the repeat domain of tau (TauRD) will serve as the effective vaccine target.

Despite the impermeability of the blood-brain barrier (BBB), multiple investigations have demonstrated the translocation of plasma immunoglobulins to the brain tissue, with their predominant internalization into neurons facilitated by low-affinity Fc receptors [26–30]. Immunoglobulins gain access to the central nervous system (CNS) by crossing compromised BBB in various neurological disorders, including Alzheimer's disease (AD) [31, 32]. Moreover, IgG can traverse the BBB through adsorption-mediated transcytosis [33]. If effective antibody responses against pathologic tau conformers are induced, there should be good chances for antibodies to prevent and resolve PHF-mediated tauopathies. Undoubtedly, for the generation of therapeutic antibodies, choosing a safe and effective epitope should be the key to success. Recent studies have suggested that soluble tau oligomers rather than insoluble aggregates are likely the most toxic species responsible for neuron cell dysfunction and death [34, 35]. Moreover, increased levels of tau oligomers have been detected in earlier stages of AD before the NFT formation and the appearance of AD clinical symptoms [36]. Therefore, specific targeting of pre-fibrillary tau oligomers should be the key to the success of AD immunotherapy. Physiological tau is a highly soluble, natively unfolded protein that stabilizes microtubules along the axonal transport track [37, 38]. Hyperphosphorylation of tau is the major trigger inducing assembly into PHFs preceding aggregation into NFTs [39, 40]. The TauRD, which includes three to four pseudo repeats, is responsible for the tau–tau-microtubule interaction, and the hexapeptide motifs ^{275}VQIINK^{280} and ^{306}VQIVYK^{311} in the four-repeat domain have been shown to initiate PHF assembly with a high tendency for β-sheet formation [41]. TauRD constitutes the majority of the microtubule-binding region in both 3R and 4R isoforms of physiological tau [16]. *In vitro* studies have also indicated that TauRD can assemble much faster than

full-length tau into PHFs independent of phosphorylation [42]. Furthermore, a truncated tau polypeptide containing the repeat domains has been found to build the core of PHFs in Alzheimer's brains [43–45]. The most advanced anti-tau vaccine AADvac1 reached phase 2 clinical trial targets a part of TauRD (^{294}KDNIKHVPGGG^{305}) in an attempt to differentially recognize pathological conformation of tau aggregates [46, 47]. This epitope was selected from a study of identifying binding epitopes of a pathological tau-specific monoclonal antibody DC8E8 that exhibited no off-target binding [48]. Considering the difficulties of extracting defined soluble oligomers from the brain and other tissues, TauRD would serve as an excellent protective epitope for AD immunotherapies.

Mucosal vaccination can trigger both humoral and cell-mediated protective immune responses in both mucosal and systemic compartments with the advantages of reduced costs, improved accessibility, needle-free delivery, and self-administration [49, 50]. Positive results have also been reported after repetitive mucosal (intranasal) administration of the Aβ peptide to transgenic mice, which induced antibodies against Aβ and partial clearance of Aβ plaques [51, 52]. Mucosal vaccines require appropriate adjuvants, as mucosally administered antigens are generally less immunogenic than those administered through systemic routes [53]. Flagellin, the structural component of flagellar filaments, is a cognate TLR5 ligand with strong mucosal adjuvant activity [54–56]. In our previous studies, we repeatedly confirmed that the *V. vulnificus* flagellin FlaB is a potent mucosal adjuvant. Intranasally administered FlaB was mostly trapped by mucosal dendritic cells (DCs) that subsequently mobilized to parafollicular areas of cervical lymph nodes and stayed there for a considerable duration [54, 57]. Brain antigens are reported to be drained into cervical lymph nodes, similar to nasally administered vaccine antigens, through the newly discovered CNS lymphatic system [58, 59], which suggests that nasal immunization may have a preference to induce immune responses against CNS-derived antigens. We hypothesized that FlaB can serve as an effective mucosal adjuvant for TauRD-based AD vaccines. In this study, we found that intranasal immunization with TauRD formulated with FlaB can induce the production of IgG antibodies specifically recognizing TauRD oligomer β-sheet aggregates while saving TauRD monomers, which would result in the prevention and resolution of pathologic PHF-tau in the tauopathic brain.

RESULTS

Development of pathologic tau conformer antigen

We hypothesized that vaccination-induced antibodies specifically recognizing pathologic tau conformers would prevent and resolve PHF-mediated tauopathies with high efficacy and safety. To establish an appropriate tau conformer antigen in PHF configuration, we selected the TauRD (2N4R-hTau amino acid 243–368) (Fig. 1A). The TauRD plays a crucial role in the hyperphosphorylation-induced PHF formation [6]. We manufactured the TauRD protein by using the pTYB12 plasmid system (Fig. 1B) and then tested whether a recombinant TauRD protein can induce PHF and NFT-resembling tangle formation. The recombinant TauRD showed a 14 kDa band on SDS PAGE, and the band could be detected by Western blot analysis using the A-10 antibody (Fig. 1C). Because NFTs constitute a quaternary (4D) protein

structure, we employed the non-denaturing native PAGE to analyze the aggregate status of TauRD. Previously, we reported that native PAGE is an explicit tool to show the quaternary conformation of proteins [60]. On the other hand, SDS PAGE would dissociate TauRD aggregates into monomer polypeptide chains. The analysis of TauRD polypeptides in native and SDS PAGE will characterize NFT-resembling TauRD aggregates and monomers, respectively. Given tau PHFs make β-sheet conformation and thioflavin S (ThS) intercalate in the β-sheet, we observed whether β-sheet PHF conformation is maintained in the native PAGE by staining with ThS. Briefly, we incubated freshly purified or heparin-treated PHF form of TauRD with ThS and carried out native PAGE. To prepare heparin-treated TauRD, TauRD proteins (in PBS) were treated with heparin (heparin sodium salt from porcine intestinal mucosa: Sigma, Cat# H3149) in a 1:8 ratio (heparin: TauRD) for 5 days at 37 ℃ without shaking. As shown in Fig. 1D, the majority of TauRD aggregates remained in the loading well or around the interface between stacking and running gels, in the presence or absence of heparin, respectively. When stained with ThS, the TauRD aggregates yielded granular bright green fluorescence, which indicated that the aggregates were composed of β-sheet structures (Fig. 1E). Heparinization of TauRD protein showed a unique ultrastructure of TauRD aggregation (Fig. 1F). This result strongly suggests that recombinant TauRD polypeptides aggregate into conformers with stable β-sheet structures, which resemble NFTs observed in tauopathy neuronal cells. The TauRD suspension in PBS was used for further animal immunization studies.

Induction of TauRD-specific antibody responses by intranasal immunizations in combination with FlaB adjuvant

We initially looked for the immunization schedule to provide stronger TauRD-specific antibody responses. Mice received intranasal immunizations consisting of 10 μg TauRD and 4 μg FlaB. To assess TauRD-specific antibody titers, serum samples obtained after three, five, and six vaccinations were analyzed using enzyme-linked immunosorbent assay (ELISA). Immunizations with TauRD + FlaB induced significantly higher levels of IgG antibody responses than TauRD alone (3-times, TauRD vs. TauRD + FlaB ** $P < 0.01$; both 5- and 6-times, TauRD vs. TauRD + FlaB ** $P < 0.001$). TauRD alone failed to induce notable antibodies compared with the group receiving the FlaB adjuvant. Six-time immunization of TauRD + FlaB induced a comparable level of antibody responses with 5-time administration ($P > 0.05$), suggesting that the ceiling of the immune response was already achieved by five immunizations.

Previous studies have demonstrated the direct binding of FlaB to human TLR5, leading to the activation of NF-κB [54, 60]. To confirm whether FlaB's immune-potentiating effect on TauRD was mediated through TLR5 signaling, we conducted a comparative analysis between BALB/c wild-type (WT) and $TLR5^{-/-}$ mice. The mice received a weekly vaccination five times, consisting of 10 μg TauRD with or without 4 μg FlaB. PBS and TauRD-only groups served as controls. In contrast to WT, the immune-potentiating effect was completely abrogated in $TLR5^{-/-}$ mice (Fig. 2). This result confirms that the immune enhancement of TauRD-specific immune responses by FlaB is indeed mediated through the host TLR5 signaling pathway

The TauRD includes four KXGS motifs that regulate microtubule affinity and aggregation kinetics. It has been reported that hyperphosphorylation of tau serves as the primary catalyst for initiating auto-assembly into PHFs, which eventually polymerize to form NFTs. The pseudo-repeats play a contributory role in the formation of β-sheet structures in pathological tau NFTs. In this context, we designed a vaccine formulation composed of those pseudo-repeat peptides as a control antigen. We employed peptide antigens consisting of $Tau_{sp}1$ (^{253}LKNVKSKIGS^{262}), $Tau_{sp}2$ (^{284}LSNVQSKCGS^{293}), $Tau_{sp}3$ (^{319}TSKCGSLGNI^{328}), and $Tau_{sp}4$ (^{347}KDRVQSKIGS^{356}) (Conserved common sequence underlined, Supplementary Table 1). Mice were intranasally immunized with the mixture of the four short peptides (Tau_{sp}mix; 25 μg each) alone or in combination with 4 μg FlaB (Tau_{sp}mix+FlaB) and evaluated TauRD-specific Ab responses. Although the antibody level was negligible after the third vaccination, the addition of FlaB to Tau_{sp}mix significantly enhanced TauRD-specific IgG antibody production after five vaccinations (*** $P < 0.001$). Notably, the Log_2 IgG titers elicited by five immunizations with Tau_{sp}mix+FlaB were significantly lower than those induced by TauRD + FlaB (7.40 ± 0.68 vs 13.40 ± 0.93, *** $P < 0.001$), despite the substantially greater total quantity of Tau_{sp}mix administered (100 μg) compared with TauRD (10 μg) (Supplementary Fig. 1).

Specific recognition of TauRD conformers by anti-TauRD + FlaB sera

Next, we characterized the antiserum obtained from mice immunized with TauRD + FlaB. Recombinant TauRD protein was subjected to separation by SDS-PAGE and subsequently transferred onto membranes for Western blot analysis. In light of Tau_{sp}mix's composition as a peptide cocktail, it is conceivable that this antigen induces antibodies with a specific affinity for amino acid sequences, rather than the pathological PHF conformation. Consequently, we utilized anti-Tau_{sp}mix+FlaB serum as a sequence-specific control. On SDS-PAGE, the TauRD aggregates near-complete dissociated into monomers, as evidenced by Ponceau S staining. The anti-Tau_{sp}mix+FlaB sera distinctively detected the TauRD monomer band. On the other hand, intriguingly, the anti-TauRD + FlaB sera exhibited negligible detection of the monomer band but displayed strong reactivity towards a higher-molecular-mass band that was not detected by Ponceau S (Supplementary Fig. 2). To confirm whether anti-TauRD + FlaB specifically recognized fibrillated TauRD, we prepared heparin-treated TauRD and performed native PAGE followed by Western blot analysis. As shown in Fig. 3A, the anti-TauRD + FlaB antibodies strongly detected aggregated TauRD within the stacking gel, whereas anti-Tau_{sp}mix+FlaB antibodies did not. Considering the Tau_{sp}mix comprises a short peptide cocktail, this antigen mixture should have induced antibodies specific to amino acid sequences, which should be hidden when pathologic conformers are formed, rather than recognizing conformational structures. These findings suggest that mice immunized with TauRD + FlaB primarily would have elicited specific antibody responses against pathologic tau conformers.

To further verify whether the anti-TauRD + FlaB serum has an affinity for PHFs, we induced fibrillization of recombinant TauRD in the presence of heparin at 37°C and harvested the fibrillized proteins at Day 2 and

Day 5 for double staining of ThS and immunofluorescence. On day 2, the TauRD protein underwent aggregation, forming PHFs that exhibited specific binding to the anti-TauRD + FlaB serum. This evident binding with intense fluorescence was exclusively colocalized with the ThS signals. By day 5, the TauRD fibrillary aggregation had further developed into dendritic tangles, which displayed stronger staining with both ThS and antibodies (Fig. 3B). To determine whether the conformer-specific antibodies present in the anti-TauRD + FlaB serum could recognize PHFs in human tauopathy lesions, we conducted immunohistochemistry (IHC) using human AD brain specimens. As a positive control, we used an anti-phospho-PHF-tau pSer202 + The205 (AT8) antibody. The conformer-specific antibodies induced by TauRD + FlaB immunization exhibited the ability to reveal intracytoplasmic neurofibrillary tangles in the human hippocampus with AD neuropathologic change (ADNC). The staining specificity was comparable to that of the commercially available pathologic Tau-specific AT8 antibody (Fig. 3C and Supplementary Fig. 3).

Interestingly, the anti-TauRD + FlaB serum exhibited recognition of tauopathic neuronal cells with significantly reduced background signals in comparison with the commercial antibody AT8. The staining intensity appeared to vary among neurodegenerative cells, whereas the AT8 antibody produced a more uniform staining pattern. Given that tauopathic degeneration within AD neuronal cells occurs at various stages in affected brain tissues, the formation of PHFs and neurofibrillary tangle is likely to be quantitatively heterogeneous. Since the anti-TauRD + FlaB serum can selectively recognize the pathologic conformation of tau PHFs, the antiserum may differentially stain neurodegenerative cells based on the level of pathologic Tau aggregates present in degenerative neuronal cells depending upon pathologic progression.

Inhibition of PHF assembly by the conformer-specific anti-TauRD + FlaB serum

Subsequently, we evaluated whether the conformer-specific polyclonal antibodies induced by multiple intranasal immunizations with TauRD + FlaB possessed the capability to inhibit TauRD tangle formation. IgG antibodies were purified from sera of mice intranasally immunized with PBS (control) or TauRD + FlaB. The purified IgG antibodies were then incubated with TauRD protein at 4°C overnight, with end-over-end rotation. Subsequently, the TauRD proteins, following incubation with the purified IgG antibodies, were subjected to aggregation for 5 days in the presence of heparin at 37°C, and the morphology of TauRD aggregates was examined by TEM. While TauRD proteins treated with control antibodies exhibited compact dendritic fibrillar tangles, the tangle formation was significantly inhibited in the presence of TauRD + FlaB IgG antibodies (Fig. 4A). This result suggests that the conformer-specific antibodies present in the anti-TauRD + FlaB sera had significantly inhibited the formation of dense tangles, rendering PHFs to disperse as shorter and thinner filaments that could be more easily phagocytosed by microglia.

Facilitation of TauRD oligomeric aggregates uptake by microglial cells with conformer-specific antibodies

Microglia, the brain's resident innate phagocytic cells, efficiently clean antibody-bound tau oligomers from the extracellular space. It has been reported that therapeutic tau antibodies can enhance the internalization of tau aggregates [61]. Hence, we investigated whether the conformer-specific antibodies targeting TauRD aggregates could facilitate the *in vitro* phagocytic degradation of TauRD aggregates by the microglial cell line BV2. Initially, we subjected the heparin-treated TauRD fibrils to sonication to fragment the TauRD tangles into smaller segments. Subsequently, we incubated BV2 cells with these TauRD tangle fragments, in the presence of anti-TauRD + FlaB serum, and subsequent phagocytosis was assessed. At 30 minutes following incubation, TauRD tangle fragments conjugated with AF555 were observed within the intracellular compartment of BV2 cells via microscopic observation (Fig. 4B). We further assessed microglial cell-mediated phagocytosis of the TauRD tangle fragments by using mouse primary microglial cells. As shown in Fig. 4C, the conformer-specific anti-TauRD + FlaB serum robustly facilitated the uptake of TauRD oligomeric aggregated by primary microglial cells. Interestingly, the phagocytosis efficiency of primary microglial cells was significantly higher than that of BV2 cells and the intensity of intracellular ThS stain decreased over time suggesting active degradation of Tau aggregates. This result suggested that the pathologic Tau conformer recognizing antibodies raised by TauRD + FlaB immunization would also induce an efficacious clearance of extracellular tau aggregates by microglia *in vivo*.

Development of a built-in adjuvanted FlaB-TauRD fusion anti-tauopathy vaccine

Next, to assess the amelioration of tauopathy progression *in vivo* by intranasal vaccination, we constructed a built-in adjuvanted vaccine comprising FlaB and TauRD (Fig. 5A). A recombinant built-in adjuvanted vaccine, fusing TauRD antigen and FlaB adjuvant as a single polypeptide, would present greater translational potential into a pharmaceutical product. The recombinant FlaB-TauRD fusion protein exhibited a single band with a molecular mass of 57 kDa on SDS-PAGE. This band was subsequently confirmed by Western blot analysis using both anti-FlaB and anti-tau (A-10) (Fig. 5B). To confirm the correct folding and functionality of the built-in adjuvanted vaccine, we checked the TLR5-stimulating activity of the FlaB-TauRD fusion protein. The FlaB-TauRD exhibited a dose-dependent TLR5-stimulating activity (Fig. 5C). Notably, the TLR-5-stimulating activity was higher, at the same stoichiometry, than that of FlaB, indicating that the fusion partner protein does not impede TLR5-binding activity and may expose even more TLR5 binding motifs.

To compare the TauRD-specific antibody responses elicited by both the mixture and built-in adjuvanted anti-tauopathy vaccines, with equimolar ratios of TauRD and FlaB, we measured TauRD-specific IgG titers in the sera. BALB/c mice received intranasal vaccinations with 3.9 μg TauRD, 3.9 μg TauRD plus 12 μg FlaB, or 15.9 μg FlaB-TauRD fusion protein, five times at one-week intervals. The results revealed comparable levels of TauRD-specific serum IgG titers between the built-in adjuvanted (FlaB-TauRD) and mixture vaccine formulation (TauRD + FlaB) (Fig. 5D). These findings encouraged us to proceed to the preclinical trial of the FlaB-TauRD fusion vaccine using a transgenic animal model.

Amelioration of tauopathy in P301S transgenic mice by mucosal immunization with FlaB-TauRD vaccine

To assess the potential of the FlaB-TauRD fusion vaccine for clinical application, we vaccinated P301S human tau transgenic mice and observed the effect of vaccination on the disease progression. In our animal facility, behavioral symptoms related to tauopathy, such as clasping and limb retractions, began to manifest approximately three months after birth. As the tauopathy advanced, we could observe deteriorating manifestations such as fur loss, limb weakness associated with the hunch-back posture, and debilitating paralysis. We assessed the presence of pathologic tau accumulation in the brain tissues of P301S mice by the immunohistochemical analysis employing an antibody specific to phosphorylated-PHF-tau at Ser202 and Thr205 (AT8). As illustrated in Supplementary Fig. 3, tauopathy progressively developed in the P301S transgenic mice over the observed time course.

To investigate the efficacy of anti-tauopathy protective immune responses elicited by the active immunization, 3- or 6-month-old P301S transgenic mice received ten intranasal immunizations with either PBS or 14 μg FlaB-TauRD every week. TauRD-specific antibody responses and the progression of tauopathy were assessed in a time course (Fig. 6A). As depicted in Figs. 6B and 6E, mice subjected to 10 times FlaB-TauRD immunization demonstrated significantly higher levels of TauRD-specific antibody titers in both 3- and 6-month-old P301S mice (*** $P < 0.001$). It was also noted that PBS-immunized P301S mice had significantly higher background anti-TauRD antibody titers compared with isogenic WT mice, suggesting endogenous transgenic P301S tau-induced notable antibody responses (Fig. 5D, 6B & E).

To assess whether the anti-FlaB-TauRD antibodies raised in P301S mice effectively inhibit tau aggregation as well, we conducted the above-mentioned *in vitro* aggregation inhibition assay. As depicted in the Supplementary Video, the anti-FlaB-TauRD sera was efficacious in inhibiting tau aggregate formation. The anti-PBS serum, which also exhibited substantial anti-TauRD antibody titer, did not exhibit any recognizable inhibition of TauRD aggregate formation. After 96 hours of incubation, robust tau aggregate formation was observed in samples treated with anti-PBS, whereas any notable aggregates were absent in samples treated with anti-FlaB-TauRD. These findings demonstrate that FlaB-TauRD vaccination induced functionally active antibodies in the P301S animals as well.

To observe whether the active immunization elicits significant phenotypic improvements in P301S mice afflicted by tauopathy, we monitored disease scores and survival as long as 70 or 40 weeks after the start of vaccination. Both 3- and 6-month-old P301S mice that received ten FlaB-TauRD immunizations exhibited significantly delayed onset of severe tauopathy signs and symptoms (*** $P < 0.001$, PBS vs. FlaB-TauRD) (Fig. 6C and 6F). Remarkably, FlaB-TauRD-immunized P301S mice exhibited significantly prolonged survival as compared to PBS-immunized counterparts in both the 3-month-old and 6-month-old P301S mice groups (** $P < 0.01$, PBS vs. FlaB-TauRD in 3-month-old mice; * $P < 0.05$, PBS vs. FlaB-TauRD in 6-month-old mice) (Fig. 6D and 6G). Earlier start (3 months) of vaccination resulted in significantly

later onset of tauopathy symptoms and longer survival though the induced antibody levels were lower than 6-month-starts (Fig. 6B-G).

To evaluate the impact of FlaB-TauRD vaccination on the behavioral traits of 6-month-old P301S mice, we conducted an open field test, a novel objective recognition test (NORT), and the Y-maze tests fourteen weeks after the last vaccination (Fig. 6H). Age-matched mice that received PBS vaccinations were evaluated as the non-vaccination control. NORT evaluates recognition memory and Y-maze tests reference memory and working memory [62]. In the NORT, the PBS-immunized group allocated a comparable amount of time to both objects (same object and novel object). In contrast, the FlaB-TauRD-immunized group spent more time inspecting the novel object than the familiar one, resulting in a higher preference index, indicative of enhanced recognition memory (**$P < 0.01$, PBS vs. FlaB-TauRD) (Fig. 6I). In the Y-maze test, which assesses impaired working memory, the FlaB-TauRD-immunized group displayed a significantly improved alternation ratio, indicative of enhanced working memory (*$P < 0.05$, PBS vs. FlaB-TauRD). Notably, there were no discernible differences in the total number of arm entries between the two groups, implying similar motor function in both groups at tested ages (Fig. 6J). The open field test revealed comparable basal locomotion activity in both the PBS- and FlaB-TauRD-immunized groups (Fig. 6K), suggesting that FlaB-TauRD immunization did not impact general motor activities between the two groups.

This outcome demonstrates that active immunization with the FlaB-TauRD vaccine engenders a protective immune response in P301S-transgenic mice, leading to improved quality of life and extended survival. In summary, these findings collectively provide compelling evidence that active immunization with the built-in adjuvanted FlaB-TauRD vaccine effectively mitigates tauopathy, ameliorating clinical and pathological aspects of the disease.

DISCUSSION

Immunotherapy against tauopathies should discriminatively target pathological tau molecules while preserving physiologically functioning ones. Immunological effectors should selectively prevent further PHF tangle formation and mediate the clearance of already-formed tau aggregates [33]. Preventing transcytosis of prion-like pathological tau seeds released from dying neuronal cells is also important to improve therapeutic efficacy [2]. In the present study, we generated a recombinant TauRD polypeptide showing a propensity toward PHF formation and tested it as an anti-tauopathy vaccine antigen in combination with the mucosal adjuvant FlaB. Notably, the antibodies induced by vaccination predominantly targeted the TauRD PHF conformers. These antibodies, which exhibit specificity for conformers, were effective in suppressing the aggregation of TauRD into tangles and facilitating the phagocytic degradation of pre-existing tangle fragments. Based upon these *in vitro* observations, we developed a built-in adjuvanted FlaB-TauRD fusion polypeptide as an anti-tauopathy vaccine and confirmed that active immunization of the FlaB-TauRD vaccine ameliorated tauopathy using the P301S human tau transgenic mouse model. This is, to our knowledge, the first report showing an efficacious

induction of antibody responses specifically targeting pathologic tau conformers and the therapeutic efficacy of TauRD PHF conformer-targeting active immunization through the intranasal route.

Tau proteins contain numerous charged residues, the net charge of 4R-TauRD at neutral pH is predicted + 10 and its isoelectric point (pI) is 10.46. It has been reported that polyanions such as heparin, RNA, and polyglutamate can enhance the efficiency of TauRD assembly by compensating the positive charges of aggregates much faster than the full-length tau protein [42, 63–65]. Even in the absence of polyanions, the recombinant TauRD polypeptide purified by the IMPACT-CN System (New England Biolabs) showed a high propensity for aggregation, as revealed by nondenaturing native PAGE, and ThS staining (Fig. 1D). Fresh recombinant TauRD protein monomers could not be separated by the native PAGE and assembled as granular structures readily stained by ThS, implicating a rather regular β sheet structure formation in buffered solutions. Different from proteins obtained from other purification systems, proteins expressed by the pTYB12 vector and purified by the IMPACT-CN System were subjected to DTT-induced on-column cleavage for 48 hours at room temperature. Given that tau assembly can be promoted by elevated temperature in a time-dependent manner [65, 66], our protein purification procedure might have contributed to the formation of TauRD oligomers and aggregates.

A recent study on epitope analysis of the tau protein pointed out the low immunogenicity of the TauRD and identified five immunogenic motifs within the N-terminal, proline-rich, and C-terminal regions of the tau protein [67]. In part, we may agree with this low-immunogenicity prediction of the TauRD since short peptide antigens or TauRD alone could not induce meaningful antibody responses even after six repeated immunizations with relatively high doses (Fig. 2 and Supplementary Fig. 1). Moreover, AADvac1 uses keyhole limpet hemocyanin (KLH)-conjugated ^{294}KDNIKHVPGGGS^{305} peptide in TauRD as the vaccine epitope, which induced significant antibody responses in animal and human subjects, in which KLH may have contributed to generate immunogenicity [46, 47]. As for short unique peptide antigens in the repeat region (Tau_{sp}mix) used in this study, adjuvanted average antibody titer after 6-time immunization was below $10Log_2$, which was supposed to be rather low to have substantial *in vivo* efficacies. On the other hand, the hypoimmunogenic TauRD, when adjuvanted with FlaB, could induce similar antibody titers to 6-time Tau_{sp}mix+FlaB immunizations even after 3-time immunizations. After 5-time immunizations, the TauRD + FlaB group reached $15Log_2$ antibody titers in a TLR5-dependent manner (Fig. 2). More interestingly, the majority, if not all, of induced Abs were able to recognize PHF tangle conformers. Compared with previously studied microbial antigens, TauRD antigen, as speculated to be relatively less immunogenic, required a higher dose and more repeated immunizations even in combination with flagellin [54, 68]. These results suggest that the TauRD + FlaB vaccine, for clinical application, should be administered regularly for a long period to maintain effective antibody titers. The immunization interval also had a significant influence on the resulting immune responses. The two-week interval was not as effective as the one-week interval (data not shown). This result indicates that more frequent and relatively higher concentrations of the presented antigen are required for effective humoral immune responses against the low-immunogenicity TauRD antigen to generate conformer-specific antibodies. Of note is the kinetics of antibody induction after vaccination. Ten micrograms of TauRD vaccine formulated with FlaB

required five immunizations to reach the ceiling level of Ab responses, although significant responses were noted after three vaccinations (Fig. 2). Given the pharmacokinetic advantages of IgG Abs and the low immunogenicity of TauRD antigen, a more repeated and frequent vaccination strategy will be required in future human trials to secure isotype switching to IgG and maintenance of therapeutic levels. TLR5 signaling through the mucosal compartment, compared with other adjuvanticity mechanisms, likely exerts a unique advantage in potentiating immune responses against TauRD epitopes. We observed that the same dose of short peptide mixture adjuvanted with complete Freund's adjuvant (CFA) failed to stimulate antibody production via subcutaneous administration (data not shown). CFA, a mixture of strong ligands for pattern recognition receptors of antigen-presenting cells and regarded as the strongest experimental adjuvant, failed to induce immune responses against short peptide TauRD antigens while FlaB induced substantial antibody responses even after three immunizations. Flagellin is also a cognate ligand of the NLRC4 inflammasome pathway [69, 70]. However, NLRC4 was supposed not to play any dominant immune-potentiating role in the present study, since the adjuvanticity was completely abolished in TLR5-KO mice. NLRC4 activation along with cytosolic antigen processing induced robust cytotoxic T lymphocyte responses [69]. A recent report noted that microglia-mediated T-cell infiltration aggravated neurodegeneration in tauopathy [71]. In this regard, the anti-tauopathy vaccine should direct the immune balance toward humoral immunity. To this end, the NLRC4 binding domain could be deleted in the development of a clinical-grade FlaB-TauRD vaccine.

An effective and safe Tau-based AD vaccine must have a high benefit/risk ratio since it will be administered to a relatively aged population that might already exhibit the beginning of neuronal degeneration. Such a vaccine must induce an adequate antibody response against pathologic tau molecules while restraining adverse responses to physiologic ones. Notably, antibodies generated in response to the FlaB-adjuvanted TauRD vaccine selectively recognized the multimeric form of TauRD (Fig. 3A and Supplementary Fig. 2). As reported, immunization of wild-type mice with full-length tau recombinant protein in complete Freund's adjuvant (CFA) and with pertussis toxin (PT) leads to tauopathy-like abnormalities and neurological deficits [17]; these are presumably related to the use of full-length human tau protein differing from the mouse sequence or the use of strong adjuvants such as CFA and PT that induce a strong cytotoxic T-cell response. The mucosal immune system has evolved a variety of mechanisms to achieve and maintain tolerance against self-antigens, and the degree of tolerance relies on the dose, route, and frequency of autoantigen administration [49]. Thus, a small proportion of monomeric TauRD administered intranasally might have been processed as tolerogenic self-antigen while the TauRD PHF conformers were recognized as foreign antigens. However, a high dose of short peptide mixture formulated with FlaB also induced the production of serum antibodies that recognized only the monomeric form of TauRD. In this case, a high dose of the short peptide mixture likely overwhelmed the tolerance of the mucosal immune system with the help of mucosal adjuvant FlaB. Accordingly, the mucosal vaccination of TauRD formulated with FlaB adjuvant likely has advantages over systemic administration regarding safety. There could be concerns about the immunogenicity of FlaB. Repeated administration will inevitably induce anti-FlaB antibodies, which may nullify TLR5-FlaB

interaction and may bring hypersensitivity reactions. To cope with this problem, we generated deimmunized FlaB by deleting the dominant B cell epitope [60, 72].

MATERIALS AND METHODS

Construction and purification of recombinant TauRD and FlaB-TauRD proteins

To generate recombinant TauRD protein, the DNA sequence encoding the 4R-tau repeat region (amino acid 243–368) from 2N4R-human tau was synthesized by Bioneer (Daejeon, Korea) (Fig. 1A). To produce a recombinant FlaB-TauRD fusion protein, we generated a pET30a + plasmid (Novagen) containing a DNA fragment encoding TauRD (amino acids 243–368) (Table 1). The insert DNA fragment was generated through PCR amplification, utilizing a codon-optimized DNA template and the following primer pair: tauRD-F and tauRD-R, with EcoRI and XhoI sites, respectively (Table 2). The detailed methods are provided in the Supplementary Information.

Table 1
Bacterial strains and plasmids used in this study

Bacteria		**Description**	**Source**
Escherichia coli DH5α	F^- *recA1* restriction negative	Laboratory collection	
E. coli ER2566	F^- λ^- *fhuA2 [lon] ompT lacZ::T7 gene1 gal sulA11Δ(mcrC-mrr)114::IS10R(mcr-73::miniTn10-TetS)2R(zgb210::Tn10)(*TetS*) endA1 [dcm]*	New England Biolabs, Inc.	
E. coli BL 21 (DE3)	*hsdS gal (λcIts857 ind1 Sam7 nin5 lacUV5-T7 gene1)*	Laboratory collection	
Plasmid			
pTYB12	N-terminal fusion expression vector in which the N terminus of a target protein is a fused Intein-tag; Ap^r	New England Biolabs, Inc.	
pET30a(+)	N-terminal fusion expression vector in which the N terminus of a target protein is a fused His-tag; Km^r	EMD Bioscience	
pTYB12::*flaB*	1.5-kb EcoRI-PstI fragment containing ORF of *flaB* cloned into pTYB12	[54]	
pTYB12::*tauRD*	378-bp EcoRI-XhoI fragment containing ORF of *tauRD* encoding the 4R-tau repeat region (amino acid 243–368) from 2N4R-human tau cloned into pTYB12	This study	
pET30a(+)::*flaB-tauRD*	pET-30a(+) plasmid containing a DNA-fragment of *flaB* fused with *tauRD* (NdeI-EcoRI-XhoI)	This study	

Table 2
PCR primers used in this study

Primer	Nucleotide sequence (5’ to 3’)
tauRD-F	CCGGAATTCCTGCAAACAGCCCCGGTTCC
tauRD-R	CCGCTCGAGATTACCTCCTCCCGGCACAT
flaB-F	GGAATTCCATATGGCAGTGAATGTAAATAC
flaB-R	CCG GAATTCGCCTAGTAGACTTAGCGCTG
The recognition sites of the restriction enzyme are indicated by underlined sequences.	

Mice

Specific pathogen-free (SPF) female BALB/c mice were purchased from the Orient Company (Seongnam, Korea). BALB/c TLR5$^{-/-}$ mice were previously characterized and described [73]. P301S-transgenic mice [B6; C3-Tg (Prnp-MAPT*P301S) PS19Vle/J] [74] were obtained from the Jackson Laboratory.

Ethics statement

All animal experimental procedures were performed with the approval of the Chonnam National University Institutional Animal Care and Use Committee under protocol CNU IACUC-H-2022-45. Maintenance of the animal research facility and experimental procedures strictly adhered to the guidelines of the Animal Welfare Act enacted by the Korean Ministry of Agriculture, Food and Rural Affairs.

Intranasal immunization

To optimize the immunization schedule, 7-week-old female BALB/c mice (OrientBio, Seongnam, Korea) were intranasally immunized as follows: PBS (control group), PBS containing 10 μg of TauRD (TauRD), and PBS containing 10 μg of TauRD plus 4 μg of FlaB (TauRD + FlaB). The final volume administered for each vaccination was 20 μl per mouse. To compare the TauRD-specific antibody responses between TauRD + FlaB and the FlaB-TauRD fusion protein, BALB/c mice were intranasally immunized as follows: PBS (control group), PBS containing 3.9 μg of TauRD (TauRD), PBS containing 3.9 μg of TauRD plus 12 μg of FlaB (TauRD + FlaB), and 14 μg of the FlaB-TauRD fusion protein. This immunization regimen was repeated five times at one-week intervals. For the active immunization of P301S mice with the FlaB-TauRD fusion protein, both male and female P301S mice aged 3 or 6 months were subjected to intranasal immunizations. These mice were administered either PBS or 14 μg of FlaB-TauRD, with a total of 10 immunizations conducted at one-week intervals.

Determination of TauRD-specific antibody titers by ELISA

The detailed methods are provided in the supplementary Information.

Western blot analysis

The detailed methods are provided in the supplementary Information.

Immunofluorescence analysis of TauRD aggregates

The purified TauRD protein was subjected to fibrillization by incubating at the concentration of 50 μM in pH 7.4 PBS at 37°C. This incubation was carried out in the presence of 2 mM dithiothreitol (DTT) (Cat# 0281-5G, VWR Life Science) and anionic cofactor heparin (heparin sodium salt from porcine intestinal mucosa, Sigma, Cat# H3149) at a ratio of 1:8 (heparin:TauRD) for 5 days at 37°C, without agitation [75]. At various time points during the incubation, protein samples were deposited onto glass coverslips that had been pre-coated with poly-D-lysine. Following fixation with 4% paraformaldehyde, these protein samples were stained using a 0.01% solution of thioflavin S (Sigma) and subsequently subjected to immunofluorescence staining. The immunofluorescence staining was carried out using TauRD anti-serum obtained from mice immunized with FlaB + TauRD, and an Alexa Fluor® 546 conjugated secondary antibody derived from goat anti-Mouse IgG (Cat# A11003, Invitrogen).

Transmission electron microscopy (TEM)

Fibrillization of the TauRD protein was initiated at 37°C in the presence of the anionic cofactor heparin, following the procedure described above. The aggregation process was allowed to proceed for either 3 or 5 days. Subsequently, solutions of the TauRD protein were diluted to a concentration of 0.1 mg/ml and applied onto carbon-coated copper grids. These grids were then subjected to staining with a 2% uranyl acetate solution. The prepared samples were examined using a transmission electron microscope (JEM −1400; JEOL Ltd., Japan) for detailed structural analysis.

Primary mouse microglial culture and TauRD aggregate uptake assays

Cortices from P0-P3 C57BL/6 mouse pups were dissected and meninges were stripped under a microscope. The cortices were mechanically dissociated by gentle pipetting. After centrifuging at 300 g for 5 min, the cells were seeded into poly-D-lysine (PDL)-coated 75-cm^2 cell culture flasks. Mixed glial cells were cultured in DMEM containing 10% FBS and 1% penicillin-streptomycin at 37°C in a 5% CO_2 incubator, with one-third of the culture medium replaced with fresh medium twice a week. The microglia were isolated from the astrocyte layer 13–16 days later by mild trypsinization [76]. The medium was centrifuged for cell pelleting. Cells were seeded onto PDL-coated coverslips in 24-well plates (1×10^5 cells /well) for immunofluorescence staining. Coverslips were washed with PBS and then fixed in 4% formaldehyde and permeabilized with 0.3% Triton X-100 in 1% BSA (bovine serum albumin). After blocking with 10% normal donkey serum in PBS, the cells were incubated with rabbit anti-Iba1 antibody (1:500, Wako, 019-19741) diluted in 1% BSA in PBS overnight at 4°C. After rinsing three times with PBS for 5 min, the cells were incubated with Alexa Fluor™ 594-conjugated donkey anti-rabbit secondary antibodies (1:500, Invitrogen, A-21207) for 1 hr at room temperature. Nuclei were counterstained with DAPI and further stained with 0.01% thioflavin S. Coverslips were then mounted with the ProLong™ Gold Antifade Mountant with DAPI.

Immunohistochemistry for brain tissue

The detailed methods are provided in the supplementary Information.

Disease scoring of P301S mice

To assess phenotypic changes following vaccination in P301S mice, disease scores were assigned based on the scoring system (Table 3). Scoring was conducted in a blinded fashion by two independent researchers utilizing the criteria, ensuring objectivity and consistency in the assessment process.

Table 3
Arbitrary disease scoring of P301S transgenic mice

Score	Characteristics
0	Normal
1	Hind leg clasping
2	Facial Alopecia
3	Hunched back
4	Hunched back with gray hair
5	Hunched back with body alopecia
6	Hunched back with body alopecia and reduced activity
8	Weak hind limb and impaired forward movement
10	Paralysis of hind limbs with impaired forward movement
11	Paralysis
12	Death

Live imaging of fibrillization inhibition by antibodies raised in P301S transgenic mice

The detailed methods are provided in the supplementary Information.

Mouse behavioral test

To perform mouse behavior tests, 6-month-old P301S mice were intranasally immunized with PBS [male (n = 3) and female (n = 5)] or 14 µg of FlaB-TauRD fusion protein [male (n = 3) and female (n = 5)] 10 times at one-week interval. Fourteen weeks after the last immunization, an open field test, a novel objective recognition test (NORT), and a Y-maze test were performed. For the open-field test, mice were let move in an open-field arena (36 × 36 cm, 40 cm high) made of hard plastic board [77]. Locomotor activity was assessed using a camera placed above the arena and an automated video tracking system (ANY-

MAZE software; Stoelting). Locomotor activity was analyzed as the total distance traveled for the first 20 minutes. NORT was performed as previously described [77]. Mice were introduced to two similar objects (A) located in the arena during training for 8 minutes [77]. After 24 hours, the mice were placed in the arena with the same object and a noble one (B). The sniffing time near each object was measured using a camera and ANY-MAZE software for 8 minutes. The preference index (%) was calculated as [new object (B) time/both objects (A + B) time] x 100. The Y-maze test was done as previously described [78]. Briefly, mice were placed in a Y-maze with 3 arms (length: 40cm, width: 5cm, height: 13cm) and allowed to freely explore the maze for 7 minutes. The number of entries to each arm was analyzed with the video tracking system (ANY-MAZE software). The alternation ratio was calculated as [the number of spontaneous alternation/total arm entries − 2] x 100. Mice with more than 5 arm entries were included in the analysis.

Statistical analysis

Statistical analyses were conducted using Prism 8.0.2 software for Windows (GraphPad Software). The results are presented as means ± standard errors of the means (SEMs) unless otherwise specified. To compare between two groups, either Student's t-test or analysis of variance (ANOVA) was employed. Survival differences were assessed for statistical significance using the Gehan-Breslow-Wilcoxon test. A *P*-value of less than 0.05 was considered statistically significant.

Declarations

Acknowledgments:

The authors thank Myeung Suk Kim and Youn Suhk Lee for their excellent technical assistance in animal and biochemical experiments.

Funding:

National Research Foundation (NRF) of Korea 2020R1A5A2031185 (JHR)

National Research Foundation (NRF) of Korea 2020M3A9G3080282 (SEL)

National Research Foundation (NRF) of Korea 2019R1A5A2027521 (SEL)

Korea Health Technology R&D Project HV22C0079 (SEL)

Author contributions:

Conceptualization: JHR, SEL, WT

Methodology: WT, JT, SHH, SP-1 (Sao Puth), SP-2 Sophea Pheng), BRM, DTN, JHR

Investigation: WT, JT, SHH, SP-1, WSC, KHL, YK, HSP

Visualization: SP-1, HSP, KHL

Funding acquisition: JHR, SEL

Project administration: JHR, SEL

Supervision: KHL, YK, MCL, WSC, SEL, JHR

Writing – original draft: WT, SP-2, KHL, HSP, SEL, JHR

Writing – review & editing: SEL, JHR

Competing interests:

Patents: Some of the data present in this article have been disclosed in the patent application published as US 10,953,082 B2, US 11,771,753 B2, JP 7269909, KR 10-2006111, and KR 10-1997319 (K.J., S.E.L., and J.H.R. listed as inventors). All other authors declare that they have no competing interests.

Data and materials availability:

All data are available in the main text or the supplementary materials.

References

1. Lee VM, Goedert M, Trojanowski JQ. Neurodegenerative tauopathies. Annual review of neuroscience. 2001;24:1121-59.
2. Li C, Gotz J. Tau-based therapies in neurodegeneration: opportunities and challenges. Nat Rev Drug Discov. 2017;16:863-83.
3. Chung DC, Roemer S, Petrucelli L, Dickson DW. Cellular and pathological heterogeneity of primary tauopathies. Mol Neurodegener. 2021;16:57.
4. Alzheimer's A. 2013 Alzheimer's disease facts and figures. Alzheimer's & dementia : the journal of the Alzheimer's Association. 2013;9:208-45.
5. Athar T, Al Balushi K, Khan SA. Recent advances on drug development and emerging therapeutic agents for Alzheimer's disease. Mol Biol Rep. 2021;48:5629-45.
6. Xia Y, Prokop S, Giasson BI. "Don't Phos Over Tau": recent developments in clinical biomarkers and therapies targeting tau phosphorylation in Alzheimer's disease and other tauopathies. Mol Neurodegener. 2021;16:37.
7. Jeganathan S, von Bergen M, Mandelkow EM, Mandelkow E. The natively unfolded character of tau and its aggregation to Alzheimer-like paired helical filaments. Biochemistry. 2008;47:10526-39.
8. Braak H, Braak E, Grundke-Iqbal I, Iqbal K. Occurrence of neuropil threads in the senile human brain and in Alzheimer's disease: a third location of paired helical filaments outside of neurofibrillary tangles and neuritic plaques. Neuroscience letters. 1986;65:351-5.

9. Khatoon S, Grundke-Iqbal I, Iqbal K. Brain levels of microtubule-associated protein tau are elevated in Alzheimer's disease: a radioimmuno-slot-blot assay for nanograms of the protein. Journal of neurochemistry. 1992;59:750-3.
10. Hardy JA, Higgins GA. Alzheimer's disease: the amyloid cascade hypothesis. Science. 1992;256:184-5.
11. Ferreira ST, Klein WL. The Abeta oligomer hypothesis for synapse failure and memory loss in Alzheimer's disease. Neurobiology of learning and memory. 2011;96:529-43.
12. Karran E, Mercken M, De Strooper B. The amyloid cascade hypothesis for Alzheimer's disease: an appraisal for the development of therapeutics. Nat Rev Drug Discov. 2011;10:698-712.
13. Goedert M. Tau protein and neurodegeneration. Seminars in cell & developmental biology. 2004;15:45-9.
14. Terry RD. Neuropathological changes in Alzheimer disease. Progress in brain research. 1994;101:383-90.
15. Giacobini E, Gold G. Alzheimer disease therapy--moving from amyloid-beta to tau. Nature reviews Neurology. 2013;9:677-86.
16. Imbimbo BP, Ippati S, Watling M, Balducci C. A critical appraisal of tau-targeting therapies for primary and secondary tauopathies. Alzheimer's & dementia : the journal of the Alzheimer's Association. 2022;18:1008-37.
17. Rosenmann H, Grigoriadis N, Karussis D, Boimel M, Touloumi O, Ovadia H, et al. Tauopathy-like abnormalities and neurologic deficits in mice immunized with neuronal tau protein. Arch Neurol-Chicago. 2006;63:1459-67.
18. Asuni AA, Boutajangout A, Quartermain D, Sigurdsson EM. Immunotherapy targeting pathological tau conformers in a tangle mouse model reduces brain pathology with associated functional improvements. The Journal of neuroscience : the official journal of the Society for Neuroscience. 2007;27:9115-29.
19. Bi M, Ittner A, Ke YD, Gotz J, Ittner LM. Tau-targeted immunization impedes progression of neurofibrillary histopathology in aged P301L tau transgenic mice. PloS one. 2011;6:e26860.
20. Chai X, Wu S, Murray TK, Kinley R, Cella CV, Sims H, et al. Passive immunization with anti-Tau antibodies in two transgenic models: reduction of Tau pathology and delay of disease progression. The Journal of biological chemistry. 2011;286:34457-67.
21. Troquier L, Caillierez R, Burnouf S, Fernandez-Gomez FJ, Grosjean ME, Zommer N, et al. Targeting phospho-Ser422 by active Tau Immunotherapy in the THYTau22 mouse model: a suitable therapeutic approach. Curr Alzheimer Res. 2012;9:397-405.
22. Gibbons GS, Kim SJ, Wu Q, Riddle DM, Leight SN, Changolkar L, et al. Conformation-selective tau monoclonal antibodies inhibit tau pathology in primary neurons and a mouse model of Alzheimer's disease. Mol Neurodegener. 2020;15:64.
23. Buee L, Bussiere T, Buee-Scherrer V, Delacourte A, Hof PR. Tau protein isoforms, phosphorylation and role in neurodegenerative disorders. Brain Res Brain Res Rev. 2000;33:95-130.

24. Boimel M, Grigoriadis N, Lourbopoulos A, Haber E, Abramsky O, Rosenmann H. Efficacy and safety of immunization with phosphorylated tau against neurofibrillary tangles in mice. Exp Neurol. 2010;224:472-85.
25. Ando K, Kabova A, Stygelbout V, Leroy K, Heraud C, Frederick C, et al. Vaccination with Sarkosyl insoluble PHF-tau decrease neurofibrillary tangles formation in aged tau transgenic mouse model: a pilot study. J Alzheimers Dis. 2014;40 Suppl 1:S135-45.
26. Fabian RH, Petroff G. Intraneuronal IgG in the central nervous system: uptake by retrograde axonal transport. Neurology. 1987;37:1780-4.
27. Fabian RH, Ritchie TC. Intraneuronal IgG in the central nervous system. Journal of the neurological sciences. 1986;73:257-67.
28. Meeker ML, Meeker RB, Hayward JN. Accumulation of circulating endogenous and exogenous immunoglobulins by hypothalamic magnocellular neurons. Brain research. 1987;423:45-55.
29. Mohamed HA, Mosier DR, Zou LL, Siklos L, Alexianu ME, Engelhardt JI, et al. Immunoglobulin Fc gamma receptor promotes immunoglobulin uptake, immunoglobulin-mediated calcium increase, and neurotransmitter release in motor neurons. Journal of neuroscience research. 2002;69:110-6.
30. Congdon EE, Gu J, Sait HB, Sigurdsson EM. Antibody uptake into neurons occurs primarily via clathrin-dependent Fcgamma receptor endocytosis and is a prerequisite for acute tau protein clearance. The Journal of biological chemistry. 2013;288:35452-65.
31. Broadwell RD, Sofroniew MV. Serum proteins bypass the blood-brain fluid barriers for extracellular entry to the central nervous system. Exp Neurol. 1993;120:245-63.
32. Zlokovic B. Can blood-brain barrier play a role in the development of cerebral amyloidosis and Alzheimer's disease pathology. Neurobiology of disease. 1997;4:23-6.
33. Zlokovic BV, Skundric DS, Segal MB, Lipovac MN, Mackic JB, Davson H. A saturable mechanism for transport of immunoglobulin G across the blood-brain barrier of the guinea pig. Exp Neurol. 1990;107:263-70.
34. Haass C, Selkoe DJ. Soluble protein oligomers in neurodegeneration: lessons from the Alzheimer's amyloid beta-peptide. Nature reviews Molecular cell biology. 2007;8:101-12.
35. Lasagna-Reeves CA, Castillo-Carranza DL, Sengupta U, Clos AL, Jackson GR, Kayed R. Tau oligomers impair memory and induce synaptic and mitochondrial dysfunction in wild-type mice. Mol Neurodegener. 2011;6:39.
36. Maeda S, Sahara N, Saito Y, Murayama S, Ikai A, Takashima A. Increased levels of granular tau oligomers: an early sign of brain aging and Alzheimer's disease. Neuroscience research. 2006;54:197-201.
37. Garcia ML, Cleveland DW. Going new places using an old MAP: tau, microtubules and human neurodegenerative disease. Current opinion in cell biology. 2001;13:41-8.
38. Gamblin TC. Potential structure/function relationships of predicted secondary structural elements of tau. Biochimica et biophysica acta. 2005;1739:140-9.

39. Alonso A, Zaidi T, Novak M, Grundke-Iqbal I, Iqbal K. Hyperphosphorylation induces self-assembly of tau into tangles of paired helical filaments/straight filaments. Proceedings of the National Academy of Sciences of the United States of America. 2001;98:6923-8.
40. Wang JZ, Grundke-Iqbal I, Iqbal K. Kinases and phosphatases and tau sites involved in Alzheimer neurofibrillary degeneration. The European journal of neuroscience. 2007;25:59-68.
41. von Bergen M, Friedhoff P, Biernat J, Heberle J, Mandelkow EM, Mandelkow E. Assembly of tau protein into Alzheimer paired helical filaments depends on a local sequence motif ((306)VQIVYK(311)) forming beta structure. Proceedings of the National Academy of Sciences of the United States of America. 2000;97:5129-34.
42. Wille H, Drewes G, Biernat J, Mandelkow EM, Mandelkow E. Alzheimer-like paired helical filaments and antiparallel dimers formed from microtubule-associated protein tau in vitro. The Journal of cell biology. 1992;118:573-84.
43. Garcia-Sierra F, Wischik CM, Harrington CR, Luna-Munoz J, Mena R. Accumulation of C-terminally truncated tau protein associated with vulnerability of the perforant pathway in early stages of neurofibrillary pathology in Alzheimer's disease. Journal of chemical neuroanatomy. 2001;22:65-77.
44. Mena R, Edwards PC, Harrington CR, MukaetovaLadinska EB, Wischik CM. Staging the pathological assembly of truncated tau protein into paired helical filaments in Alzheimer's disease. Acta Neuropathol. 1996;91:633-41.
45. Wischik CM, Novak M, Thogersen HC, Edwards PC, Runswick MJ, Jakes R, et al. Isolation of a fragment of tau derived from the core of the paired helical filament of Alzheimer disease. Proceedings of the National Academy of Sciences of the United States of America. 1988;85:4506-10.
46. Novak P, Kovacech B, Katina S, Schmidt R, Scheltens P, Kontsekova E, et al. ADAMANT: a placebo-controlled randomized phase 2 study of AADvac1, an active immunotherapy against pathological tau in Alzheimer's disease. Nat Aging. 2021;1:521-34.
47. Kontsekova E, Zilka N, Kovacech B, Novak P, Novak M. First-in-man tau vaccine targeting structural determinants essential for pathological tau-tau interaction reduces tau oligomerisation and neurofibrillary degeneration in an Alzheimer's disease model. Alzheimers Res Ther. 2014;6:44.
48. Kontsekova E, Zilka N, Kovacech B, Skrabana R, Novak M. Identification of structural determinants on tau protein essential for its pathological function: novel therapeutic target for tau immunotherapy in Alzheimer's disease. Alzheimers Res Ther. 2014;6:45.
49. Holmgren J, Czerkinsky C. Mucosal immunity and vaccines. Nat Med. 2005;11:S45-53.
50. Brandtzaeg P. Function of mucosa-associated lymphoid tissue in antibody formation. Immunological investigations. 2010;39:303-55.
51. Weiner HL, Lemere CA, Maron R, Spooner ET, Grenfell TJ, Mori C, et al. Nasal administration of amyloid-beta peptide decreases cerebral amyloid burden in a mouse model of Alzheimer's disease. Annals of neurology. 2000;48:567-79.
52. Spooner ET, Desai RV, Mori C, Leverone JF, Lemere CA. The generation and characterization of potentially therapeutic Abeta antibodies in mice: differences according to strain and immunization

protocol. Vaccine. 2002;21:290-7.
53. Rhee JH. Current and New Approaches for Mucosal Vaccine Delivery. Mucosal Vaccines. 2020:325-56.
54. Lee SE, Kim SY, Jeong BC, Kim YR, Bae SJ, Ahn OS, et al. A bacterial flagellin, Vibrio vulnificus FlaB, has a strong mucosal adjuvant activity to induce protective immunity. Infect Immun. 2006;74:694-702.
55. Hong SH, Byun YH, Nguyen CT, Kim SY, Seong BL, Park S, et al. Intranasal administration of a flagellin-adjuvanted inactivated influenza vaccine enhances mucosal immune responses to protect mice against lethal infection. Vaccine. 2012;30:466-74.
56. Applequist SE, Rollman E, Wareing MD, Liden M, Rozell B, Hinkula J, et al. Activation of innate immunity, inflammation, and potentiation of DNA vaccination through mammalian expression of the TLR5 agonist flagellin. Journal of immunology. 2005;175:3882-91.
57. Lee SE, Hong SH, Verma V, Lee YS, Duong TN, Jeong K, et al. Flagellin is a strong vaginal adjuvant of a therapeutic vaccine for genital cancer. Oncoimmunology. 2016;5:e1081328.
58. Aspelund A, Antila S, Proulx ST, Karlsen TV, Karaman S, Detmar M, et al. A dural lymphatic vascular system that drains brain interstitial fluid and macromolecules. J Exp Med. 2015;212:991-9.
59. Engelhardt B, Vajkoczy P, Weller RO. The movers and shapers in immune privilege of the CNS. Nat Immunol. 2017;18:123-31.
60. Khim K, Bang YJ, Puth S, Choi Y, Lee YS, Jeong K, et al. Deimmunization of flagellin for repeated administration as a vaccine adjuvant. NPJ Vaccines. 2021;6:116.
61. Funk KE, Mirbaha H, Jiang H, Holtzman DM, Diamond MI. Distinct Therapeutic Mechanisms of Tau Antibodies: Promoting Microglial Clearance Versus Blocking Neuronal Uptake. The Journal of biological chemistry. 2015;290:21652-62.
62. Webster SJ, Bachstetter AD, Nelson PT, Schmitt FA, Van Eldik LJ. Using mice to model Alzheimer's dementia: an overview of the clinical disease and the preclinical behavioral changes in 10 mouse models. Front Genet. 2014;5:88.
63. Goedert M, Jakes R, Spillantini MG, Hasegawa M, Smith MJ, Crowther RA. Assembly of microtubule-associated protein tau into Alzheimer-like filaments induced by sulphated glycosaminoglycans. Nature. 1996;383:550-3.
64. Perez M, Valpuesta JM, Medina M, deGarcini EM, Avila J. Polymerization of tau into filaments in the presence of heparin: The minimal sequence required for tau-tau interaction. Journal of neurochemistry. 1996;67:1183-90.
65. Friedhoff P, Schneider A, Mandelkow EM, Mandelkow E. Rapid assembly of Alzheimer-like paired helical filaments from microtubule-associated protein tau monitored by fluorescence in solution. Biochemistry. 1998;37:10223-30.
66. Kumar S, Tepper K, Kaniyappan S, Biernat J, Wegmann S, Mandelkow EM, et al. Stages and Conformations of the Tau Repeat Domain during Aggregation and Its Effect on Neuronal Toxicity. Journal of Biological Chemistry. 2014;289:20318-32.

67. Selenica MLB, Davtyan H, Housley SB, Blair LJ, Gillies A, Nordhues BA, et al. Epitope analysis following active immunization with tau proteins reveals immunogens implicated in tau pathogenesis. J Neuroinflamm. 2014;11.
68. Puth S, Hong SH, Na HS, Lee HH, Lee YS, Kim SY, et al. A built-in adjuvant-engineered mucosal vaccine against dysbiotic periodontal diseases. Mucosal Immunol. 2019;12:565-79.
69. Puth S, Verma V, Hong SH, Tan W, Lee SE, Rhee JH. An all-in-one adjuvanted therapeutic cancer vaccine targeting dendritic cell cytosol induces long-lived tumor suppression through NLRC4 inflammasome activation. Biomaterials. 2022;286:121542.
70. Zhao Y, Yang J, Shi J, Gong YN, Lu Q, Xu H, et al. The NLRC4 inflammasome receptors for bacterial flagellin and type III secretion apparatus. Nature. 2011;477:596-600.
71. Chen X, Firulyova M, Manis M, Herz J, Smirnov I, Aladyeva E, et al. Microglia-mediated T cell infiltration drives neurodegeneration in tauopathy. Nature. 2023;615:668-77.
72. Rhee JH, Khim K, Puth S, Choi Y, Lee SE. Deimmunization of flagellin adjuvant for clinical application. Curr Opin Virol. 2023;60:101330.
73. Uematsu S, Fujimoto K, Jang MH, Yang BG, Jung YJ, Nishiyama M, et al. Regulation of humoral and cellular gut immunity by lamina propria dendritic cells expressing Toll-like receptor 5. Nat Immunol. 2008;9:769-76.
74. Yoshiyama Y, Higuchi M, Zhang B, Huang SM, Iwata N, Saido TC, et al. Synapse loss and microglial activation precede tangles in a P301S tauopathy mouse model. Neuron. 2007;53:337-51.
75. von Bergen M, Barghorn S, Li L, Marx A, Biernat J, Mandelkow EM, et al. Mutations of tau protein in frontotemporal dementia promote aggregation of paired helical filaments by enhancing local beta-structure. The Journal of biological chemistry. 2001;276:48165-74.
76. Saura J, Tusell JM, Serratosa J. High-yield isolation of murine microglia by mild trypsinization. Glia. 2003;44:183-9.
77. Choi WS, Kim HW, Tronche F, Palmiter RD, Storm DR, Xia Z. Conditional deletion of Ndufs4 in dopaminergic neurons promotes Parkinson's disease-like non-motor symptoms without loss of dopamine neurons. Sci Rep. 2017;7:44989.
78. Jeong J, Park HJ, Mun BR, Jang JK, Choi YM, Choi WS. JBPOS0101 regulates amyloid beta, tau, and glial cells in an Alzheimer's disease model. PloS one. 2020;15:e0237153.

Figures

Figure 1

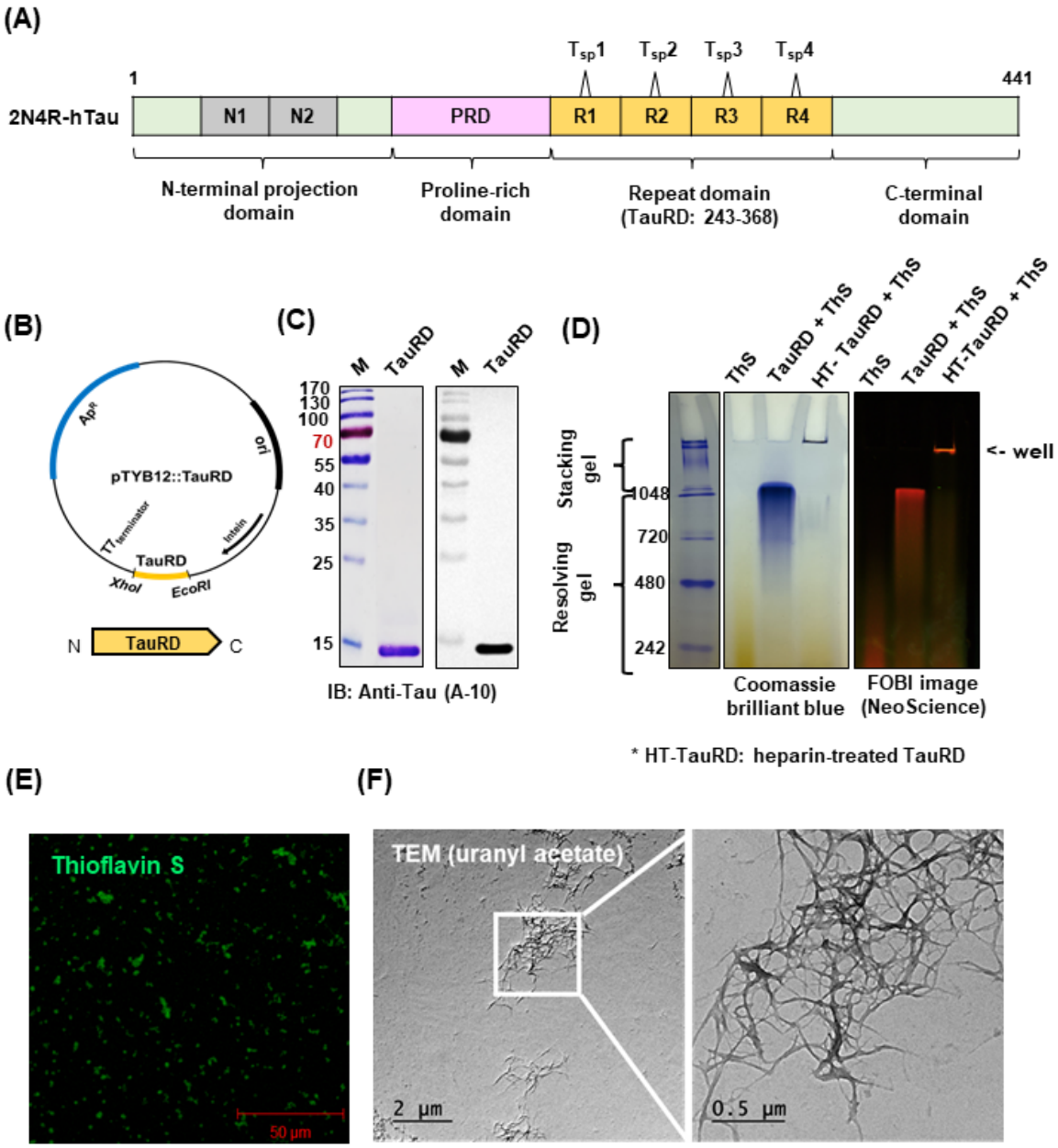

Figure 1

Development of TauRD antigen. (A) Schematic representation of human 2N4R-tau with annotations of functional domains (TauRD) and four selected short peptides. The depicted diagram illustrates the structural organization of human 2N4R-tau, with amino acid residues indicated by numbers (243-368) representing the recombinant TauRD polypeptide. **(B)** Construction of an expression vector for TauRD antigen. Depicted in this figure are DNA fragments representing the tau repeat domain (TauRD), the intein

tag gene, the T7 promoter region, the ampicillin resistance gene (Ap), and the cloning restriction enzyme sites. **(C)** Analysis of Purified Recombinant TauRD by SDS-PAGE and Western Blot. Recombinant TauRD proteins were resolved using SDS-PAGE, and subsequently, the TauRD protein bands were detected and visualized using the tau (A-10) antibody obtained from Santa Cruz Biotechnology (cat. sc-390476). **(D)** Native-PAGE analysis of purified recombinant TauRD and heparin-treated TauRD aggregates. Twenty μg of TauRD or heparin-treated TauRD fibrils were incubated with 3.1 mM Thioflavin S (ThS) for 15 minutes at room temperature, maintaining a TauRD:Thioflavin S ratio of 5:1. The samples were subsequently mixed with native loading buffer (comprising 60 mM Tris-HCl, 25% glycerol, and 0.1% Bromophenol blue) and loaded into a 10% Native-PAGE gel. Gel imaging was performed using a fluorescence-labeled organism bioimaging instrument (FOBI; NeoScience). **(E)** Confocal microscopic observation of aggregated TauRD with Thioflavin S staining. This figure illustrates the results of confocal microscopy for the observation of aggregated TauRD. Thioflavin S staining was employed to confirm the presence of a β-sheet structure within the TauRD aggregates. **(F)** Transmission Electron micrographs of TauRD proteins aggregated via heparinization. The process of fibrillization of TauRD protein was initiated at 37°C in the presence of the anionic cofactor heparin, with a molar ratio of TauRD to heparin set at 8:1. The aggregation was allowed to proceed for 3 days.

Figure 2

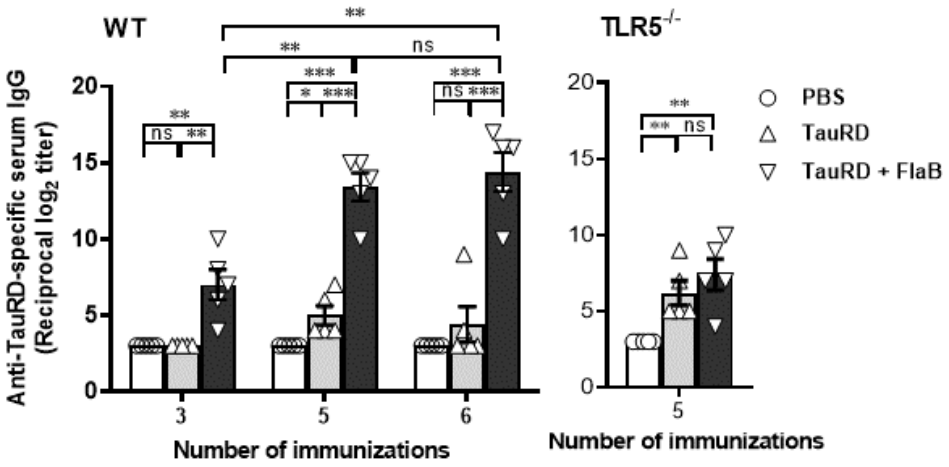

Figure 2

Antigen-specific antibody response following intranasal immunization of FlaB-adjuvanted TauRD. Wild-type BALB/c or TLR5 KO (BALB/c background) mice were subjected to intranasal administration of one of the following at one-week intervals: PBS, PBS containing 10 μg of TauRD, or PBS containing 10 μg of TauRD in combination with 4 μg of FlaB (TauRD+FlaB). Following the third, fifth, and sixth immunizations, levels of TauRD-specific serum IgG were evaluated using enzyme-linked immunosorbent

assay (ELISA). Statistical differences were analyzed by the Student's t-test for unpaired means. *$P < 0.05$, **$P < 0.01$, ***$P < 0.001$, ^{ns} not significant. The error bars represent the standard error of the mean (SEM) values.

Figure 3

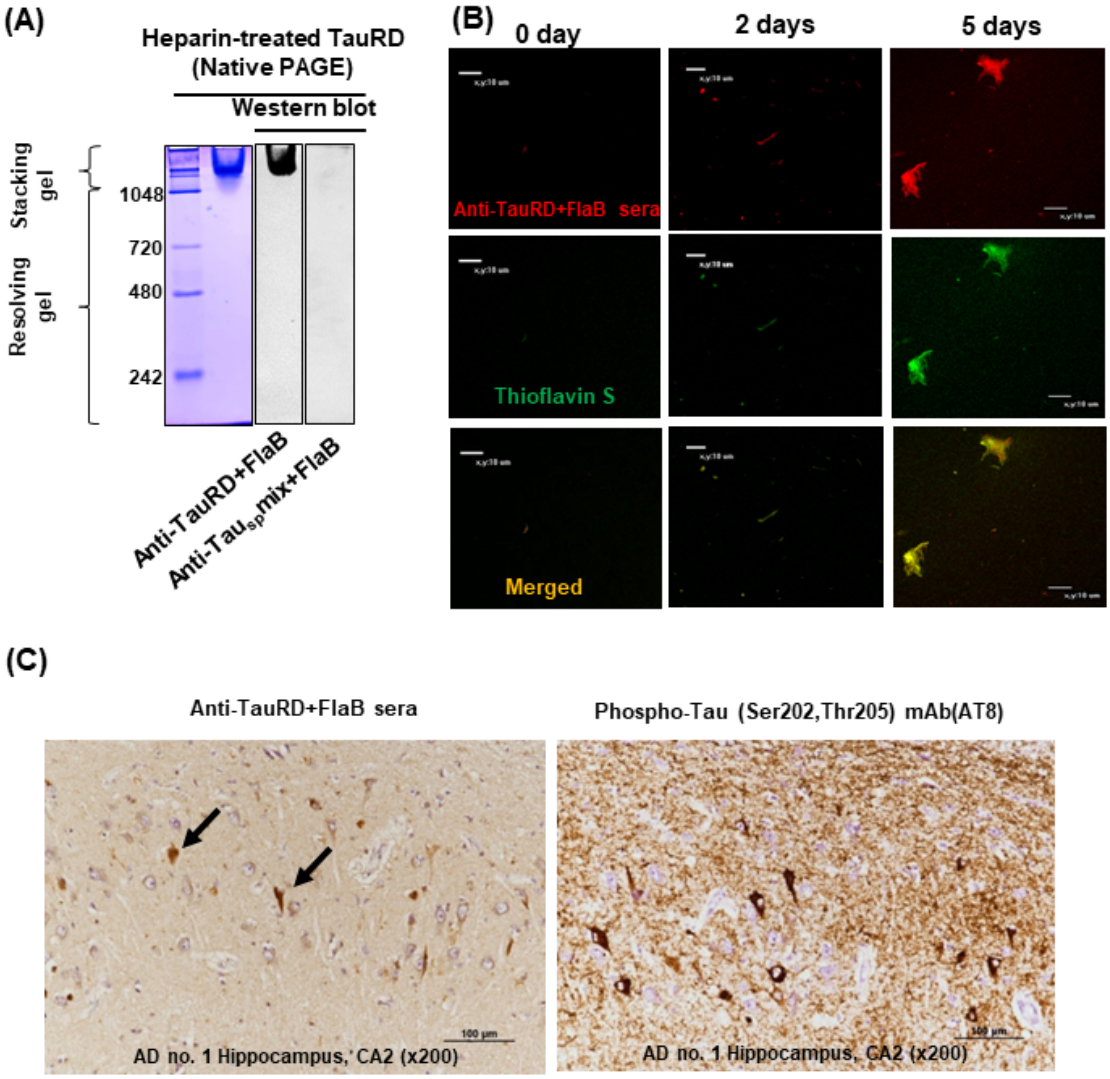

Figure 3

Characterization of anti-TauRD+FlaB sera induced by repeated intranasal immunization. (A) Immunoblot analysis of heparin-treated TauRD aggregates separated by native PAGE using Anti-TauRD+FlaB sera induced by repeated intranasal immunization. Heparinized TauRD proteins were resolved using native-PAGE, and subsequently, the TauRD protein bands were detected and visualized using the anti-sera induced by intranasal immunization with TauRD and FlaB (1:500 dilution). Postimmune serum obtained from the Tau_{sp}mix+FlaB group was employed as an antibody capable of recognizing the sequence-specific tau protein, with a 1:200 dilution. **(B)** Immunofluorescence detection of heparin-treated TauRD aggregates using anti-TauRD+FlaB sera induced by intranasal immunization. Heparin-treated TauRD fibrils were double stained with thioflavin S and postimmune serum from the FlaB+TauRD group. **(C)** Immunohistochemical detection of human Alzheimer's disease tauopathy specimen using anti-TauRD+FlaB sera induced by intranasal immunization. Immunohistochemistry of anti-TauRD+FlaB serum showed strong and specific staining in the neurofibrillary tangles of the hippocampi of humans with Alzheimer's disease (black arrows). The staining was compared with IHC by phospho-PHF-tau pSer202+The205 antibody (AT8; Invitrogen) in the sequential sections from the same case of Alzheimer's disease.

Figure 4

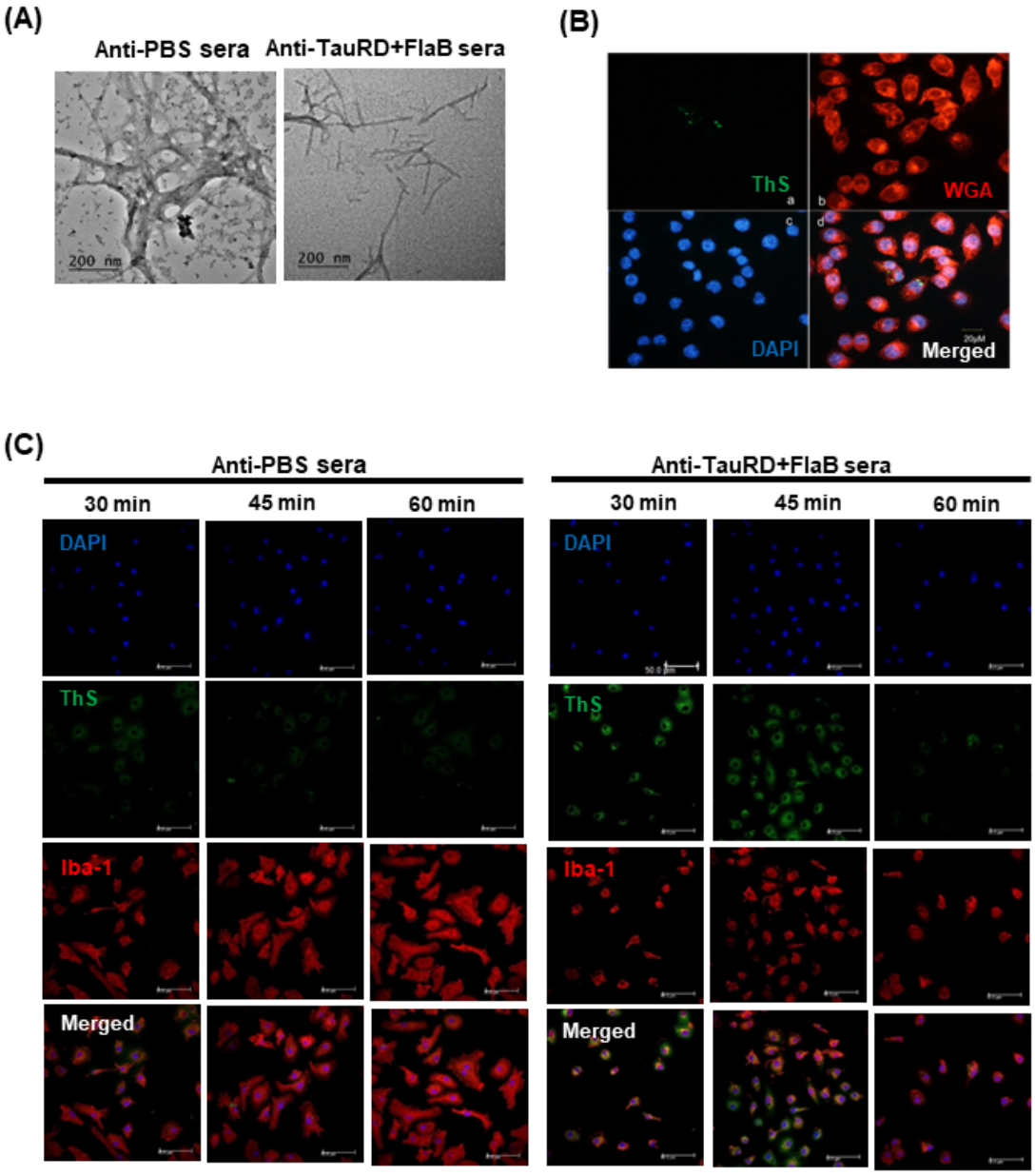

Figure 4

Functional characteristics of anti-TauRD+FlaB sera induced by repeated intranasal immunization. (A) TEM analysis of TauRD aggregation in the presence of anti-TauRD+FlaB sera induced by intranasal immunization. TauRD protein was pretreated with either anti-PBS or anti-TauRD+FlaB sera and then induced to aggregate for 5 days in the presence of heparin. Fluorescence micrographs **(B)** demonstrating the uptake of TauRD aggregates by BV2 Cells. Heparin-treated TauRD fibrils were first sonicated, followed

by incubation with anti-TauRD+FlaB or anti-PBS sera. Subsequently, BV2 cells were treated with the TauRD-antisera complex. (C) TauRD aggregate uptake in the primary mouse microglial culture. Mouse microglial cells were prepared and then the cells were treated with TauRD-antisera complex.

Figure 5

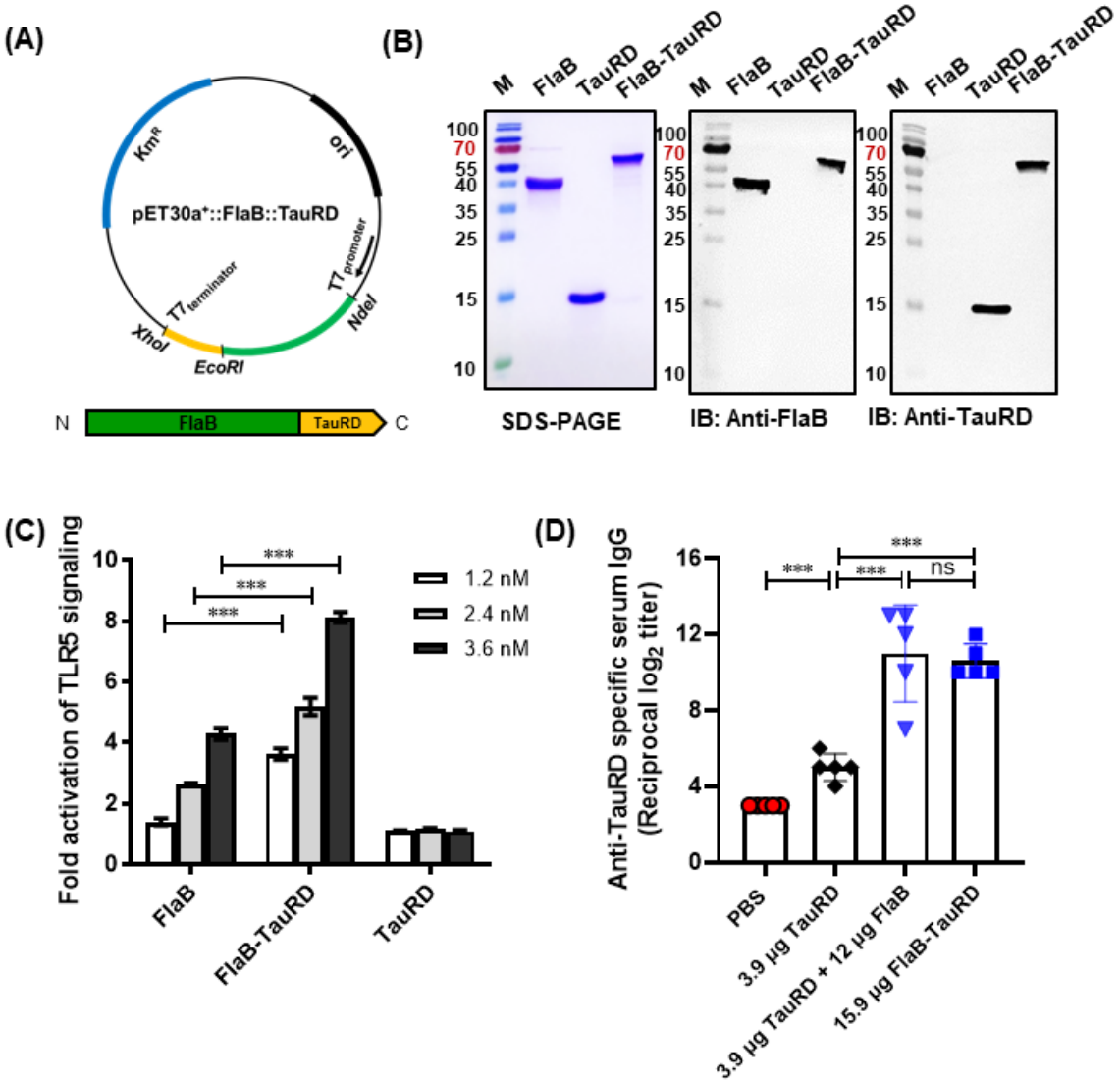

Figure 5

Generation and characterization of the built-in adjuvanted FlaB-TauRD vaccine. (A) Construction of the expression vector for the built-in adjuvanted FlaB-TauRD vaccine. DNA fragments of Vv-flaB, TauRD, the T7 promoter region, a kanamycin resistance gene (Km), and cloning restriction enzyme sites are shown. **(B)** SDS PAGE and Western blot analysis of the purified recombinant FlaB-TauRD fusion protein. The FlaB-TauRD protein was probed with an anti-FlaB or anti-TauRD antibody whose production was elicited by intraperitoneal injection of FlaB or TauRD in combination with Freund's adjuvant. **(C)** Determination of TLR5-dependent NF-κB stimulating activity by FlaB-TauRD. The relative luciferase activity levels in the cell extracts were analyzed by a dual-luciferase reporter assay system and normalized using the pCMV-β-galactosidase plasmid as a control. The same molar ratios of proteins were used, and PBS was used as a negative control. **(D)** Comparison of TauRD-specific Ab titers between anti-TauRD+FlaB and anti-FlaB-TauRD antiserum. Statistical differences were analyzed by the Student's t-test for unpaired means. $*P < 0.05$, $**P < 0.01$, $***P < 0.001$, ^{ns} not significant. The error bars represent the standard error of the mean (SEM) values.

Figure 6

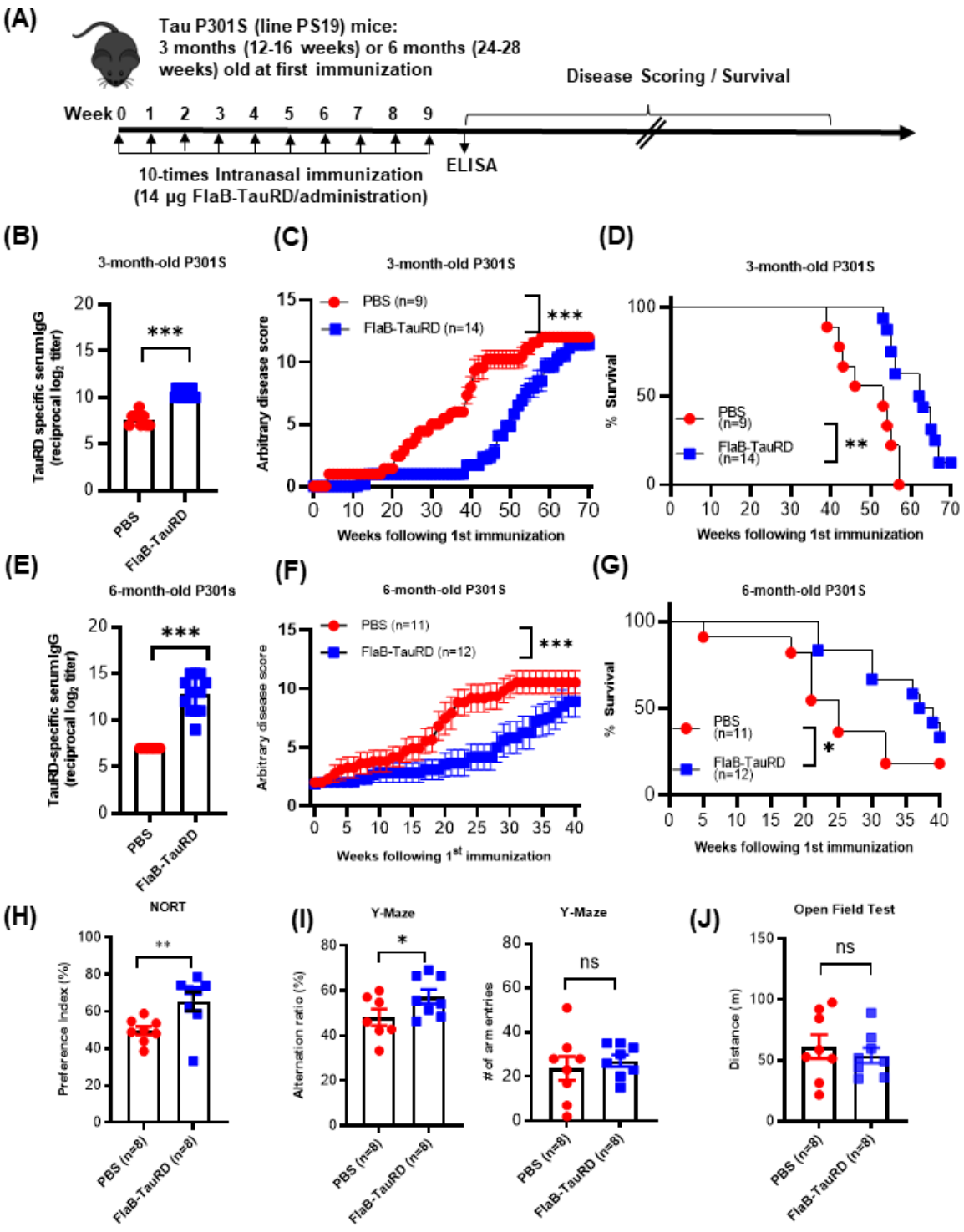

Figure 6

Amelioration of tauopathy in P301S-transgenic mice through active immunization with the built-in adjuvanted FlaB-TauRD vaccine. **(A)** Experimental schedule of multiple immunizations with recombinant FlaB-TauRD fusion protein. At the age of either three or six months, P301S mice were intranasally immunized with either phosphate-buffered saline (PBS) or 14 µg of FlaB-TauRD at weekly intervals for a total of ten times. **(B, E)** TauRD-specific serum IgG levels following ten-times intranasal immunization of

FlaB-adjuvanted TauRD. One week after the final immunization, levels of TauRD-specific serum IgG were evaluated using enzyme-linked immunosorbent assay (ELISA). **(C, F)** Determination of the disease score of tauopathy in P301S-transgenic mice. **(D, G)**Measurement of survival of vaccinated mice. Following the multiple rounds of immunization, the disease score and survival of the immunized P301S mice were assessed. **(H)** Experimental schedule of behavior tests. Fourteen weeks following the tenth immunization, a Novel Objective Recognition Test (NORT) **(I),** the Y-maze tests **(J),** and an open field test **(K)** were carried out.

Supplementary Files

This is a list of supplementary files associated with this preprint. Click to download.

- TauNVSupplementaryMaterials20231130.docx
- TauVaccineSupplFigures20231130.pptx
- Video1AAntiPBS.mp4
- Video1BAntiFlaBTauRD.mp4